Article

# Oldest thylakoids in fossil cells directly evidence oxygenic photosynthesis

https://doi.org/10.1038/s41586-023-06896-7

Received: 25 May 2023

Accepted: 23 November 2023

Published online: 3 January 2024

Check for updates

Catherine F. Demoulin[1]✉, Yannick J. Lara[1], Alexandre Lambion[1] & Emmanuelle J. Javaux[1]✉

Today oxygenic photosynthesis is unique to cyanobacteria and their plastid relatives within eukaryotes. Although its origin before the Great Oxidation Event is still debated[1–4], the accumulation of $O_2$ profoundly modified the redox chemistry of the Earth and the evolution of the biosphere, including complex life. Understanding the diversification of cyanobacteria is thus crucial to grasping the coevolution of our planet and life, but their early fossil record remains ambiguous[5]. Extant cyanobacteria include the thylakoid-less *Gloeobacter*-like group and the remainder of cyanobacteria that acquired thylakoid membranes[6,7]. The timing of this divergence is indirectly estimated at between 2.7 and 2.0 billion years ago (Ga) based on molecular clocks and phylogenies[8–11] and inferred from the earliest undisputed fossil record of *Eoentophysalis belcherensis*, a 2.018–1.854 Ga pleurocapsalean cyanobacterium preserved in silicified stromatolites[12,13]. Here we report the oldest direct evidence of thylakoid membranes in a parallel-to-contorted arrangement within the enigmatic cylindrical microfossils *Navifusa majensis* from the McDermott Formation, Tawallah Group, Australia (1.78–1.73 Ga), and in a parietal arrangement in specimens from the Grassy Bay Formation, Shaler Supergroup, Canada (1.01–0.9 Ga). This discovery extends their fossil record by at least 1.2 Ga and provides a minimum age for the divergence of thylakoid-bearing cyanobacteria at roughly 1.75 Ga. It allows the unambiguous identification of early oxygenic photosynthesizers and a new redox proxy for probing early Earth ecosystems, highlighting the importance of examining the ultrastructure of fossil cells to decipher their palaeobiology and early evolution.

Cyanobacteria have played an important part in the evolution of early life and Earth, as one of the major actors in the Great Oxidation Event (GOE) around 2.4 billion years ago (Ga) and possible but disputed earlier low-oxygenation events, based on the geochemical record[2–4]. Phylogeny of enzymes involved in the use or production of $O_2$ suggests an early availability of oxygen at around 3.1 Ga (ref. 14), whereas phylogenetic analyses of PSII genes suggest that an early form of oxygenic photosynthesis was established by 3.0 Ga (refs. 15,16). However, the appearance of oxygenic photosynthesis does not need to coincide with the origin of crown cyanobacteria, which diversified before[17,18] or after[19] the GOE. Cyanobacteria diverged from non-photosynthetic relatives between 3.37 and 2.54 Ga based on molecular clock estimates, and crown group cyanobacteria diverged from their stem relatives before or after the GOE (3.67–2.02 Ga)[1]. These early redox fluctuations led to the development of new oxygenated ecological niches in which aerobe life, including eukaryotes, diversified, leading to complex ecosystems. Cyanobacteria are also the ancestors of the chloroplast[20], the organelle in which oxygenic photosynthesis takes place within eukaryotes, which enabled the diversification of photosynthetic protists, multicellular algae and, later, plants. Despite their importance, their unambiguous fossil record remains to be evidenced. Although simple filamentous and coccoidal fossils that are abundant in Proterozoic shales and cherts are usually—and probably rightly—attributed to cyanobacteria, their simple morphology and occurrence in the photic zone of aquatic deposits are not unique to these microorganisms[5]. To date, only four microfossil taxa are interpreted with confidence as cyanobacteria, including 2.018–1.854 Ga (ref. 13) *Eoentophysalis belcherensis*, the oldest fossil interpreted as a cyanobacterium[5,12,21,22]; the endolithic Pleurocapsales 1.35–1.01 Ga *Polybessurus*[23] and 1.63 Ga *Eohyella*[24]; and a 1.040–1.006 Ga Nostocales Stigonemataceae cyanobacterium *Polysphaeroides filiformis* (C.F.D. et al., manuscript in preparation). These microfossils are identified based on their particular morphology and division pattern, and their habitat, except for *P. filiformis*, unambiguously identified as a cyanobacterium thanks to a combination of morphological, chemical and ultrastructural features (C.F.D. et al., manuscript in preparation).

In combination with morphology, ecology and chemistry, one criterion that is scarcely used to identify microfossils—although it may provide crucial palaeobiological information—is the ultrastructure of cell walls and intracellular organelles (C.F.D. et al., manuscript in preparation)[25,26]. Thylakoids represent direct ultrastructural evidence for oxygenic photosynthesis metabolism. Thylakoid membranes are dense, mostly galactolipid, protein-containing bilayers in which photosynthesis occurs in photosynthetic organisms. They have a tridimensional lamellar organization in cyanobacterial cells or in the chloroplast of algae and plants. When present in cyanobacteria, thylakoids are found in different arrangements in the cell lumen, whereas

[1]Early Life Traces & Evolution-Astrobiology, UR Astrobiology, University of Liège, Liège, Belgium. ✉e-mail: cdemoulin@uliege.be; ej.javaux@uliege.be

in eukaryotes they are compacted within chloroplasts in two types of structure, the grana and stroma lamellar domains[27]. Thylakoid arrangement in cyanobacteria can be parietal, radial, fascicular, irregular or parallel to the cell membrane[28,29]. Their origin postdates the emergence of crown cyanobacteria. Indeed, the earliest diverging extant cyanobacterial lineage, the genus *Gloeobacter*, characterized by the absence of thylakoids[6,30], is placed at the most basal position in phylogenetic reconstructions[17,31], which suggests that this lineage may have conserved traits inherited from the ancestral lineage of cyanobacteria[32]. The recent discovery of a second thylakoid-less cyanobacterial genus, *Anthocerotibacter*, was used to estimate divergence with *Gloeobacter* around 1.4 Ga (ref. 10).

One recent hypothesis suggested that the early emergence of thylakoid-forming cyanobacteria may partly explain the span of the GOE by 'multiplier effect'[33]. This proposition holds on the expansion of the photosynthetic surface by the multilayered photosynthetic membranes inside the cells that allow a higher production of $O_2$ in comparison with the smaller surface of the sole cell membrane that hosts the photosynthetic machinery in *Gloeobacter*-type cyanobacteria[32]. In contrast with this hypothesis, other authors have suggested the emergence of crown group cyanobacteria (which includes both thylakoid-less and thylakoid-forming cyanobacteria) after the GOE[9], illustrating the debates around the early evolution of cyanobacteria.

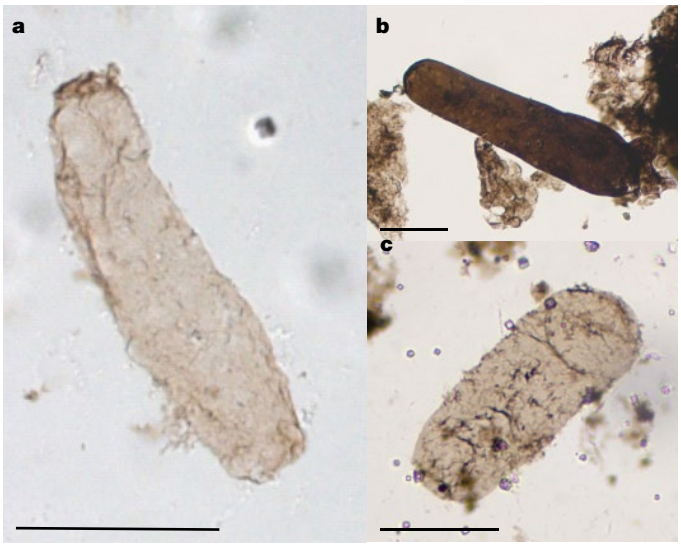


**Fig. 1 | Images of *N. majensis* microfossils. a**, *N. majensis* ($n = 16$) from the McDermott Formation, Tawallah Supergroup, northern Australia. **b**, *N. majensis* ($n = 22$) from the Grassy Bay Formation, Shaler Supergroup, Arctic Canada. **c**, *N. majensis* ($n = 13$) from the BIIc6 Formation, Mbuji-Mayi Supergroup, DRC. One representative specimen for each formation. *n*, number of measured specimens. Scale bars, 50 µm.

## Fossil thylakoids

In the fossil record, thylakoids were identified in 0.152–0.157 Ga microfossils from Kimmeridgian bituminous shales[34]. These structures interpreted as thylakoids are linear or contorted, with sharp outlines and a thickness of 35–70 nm (ref. 34). Thylakoidal structures were also reported in potential algal aggregates from the Late Ediacaran (0.55 Ga)[35]. In younger samples, chloroplasts have been identified in various fossil plants of the Cenozoic[36,37]. The preservation of thylakoids extracted by acid demineralization was also reported in 600-year-old cyanobacterial mats from Antarctic lacustrine sediments[38].

Here we report the presence of thylakoids in the microfossil *Navifusa majensis*, an enigmatic, ellipsoidal, organic-walled microfossil known in Mesoproterozoic to Neoproterozoic assemblages, although other species of the genus range up to the Carboniferous[39]. Its taxonomic identity is unresolved and probably polyphyletic, as such a simple shape is known in diverse clades. The specimens studied here are preserved as carbonaceous compressions in shales of the 1.78–1.73 Ga McDermott Formation, Australia, the 1.01–0.90 Ga Grassy Bay Formation, Arctic Canada and the 1.040–1.006 Ga BIIc6 Formation, Democratic Republic of the Congo (DRC). This mode of fossilization as thin carbonaceous compressions is common throughout the geological record for organic-walled microfossils that are flattened within fine-grained, clay-rich, layered sediments[5,22,25,26,37]. The presence of thylakoids in the Proterozoic fossil record was previously indirectly inferred from the record of microfossil taxa identified unambiguously as late Palaeoproterozoic and younger cyanobacteria or late Mesoproterozoic algae, but never observed. Here we present direct evidence for the preservation of thylakoids within fossil cells and suggest a minimum age for the emergence of thylakoid-bearing cyanobacteria before 1.75 Ga, consistent with the fossil record of unambiguous cyanobacteria.

## Ultrastructure of *N. majensis*

Specimens *of N. majensis* from (1) laminated grey shales of the 1.78–1.73 Ga, shallow-water, marine-to-estuarine/fluviatile McDermott Formation of the Tawallah Group, McArthur basin, northern Australia[40], (2) the 1.01–0.90 Ga, shallow-water estuarine Grassy Bay Formation of the Shaler Supergroup, from the Brock Inlier in the Northwest Territories of Arctic Canada[26] and (3) the 1.040–1.006 Ga (ref. 41), shallow-water marine BIIc6 Formation of the Mbuji-Mayi Supergroup, DRC[42] were analysed in this study. These consist of organic-walled, unornamented, non-septate, ellipsoidal vesicles with rounded, closed ends[43] (Fig. 1). Their size range overlaps, with McDermott specimens ($n = 16$) that are 57–177 µm in length and 17–40 µm in width; Grassy Bay specimens ($n = 22$) that are 84–264 µm in length and 23–53 µm in width; BIIc6 Mbuji-Mayi specimens ($n = 13$) that are 75–183 µm in length and 34–60 µm in width; and specimens from the Bylot Supergroup measured in Hofmann and Jackson[44]. The ultrastructure of unstained, resin-embedded specimens was observed with transmission electron microscopy (TEM) through transversal ultrathin sections. Because these organic-walled microfossils are preserved as thin carbonaceous compressions in fine-grained sediments, the length of transversal TEM sections corresponds to the width of the microfossils, whereas the thickness corresponds to that of the compressed microfossils (Extended Data Fig. 4). *N. majensis* specimens from the Tawallah Group show a set of intracellular membranes with sharp, darker edges that appear to be either parallel to the cell wall or locally contorted (Fig. 2a,b). Each membrane comprises one medium-electron-dense layer surrounded by two electron-dense layers (Fig. 2a,b). These membranes have a thickness ranging from 10 to 20 nm (Extended Data Fig. 3 and Extended Data Table 1). The cell wall consists of one electron-lucent layer and one thin electron-dense layer with a total thickness of up to 70 nm (Fig. 2b). The cell wall has an irregular thickness all along the section and is sometimes poorly preserved. The inner membranes are not stored in compartments such as chloroplasts and do not show grana or stroma lamellae-like structures, implying that these fossils are not eukaryotic[45]. Indeed, in the chloroplast, stacked concentric layers are all surrounded by the plastid wall, a concentric bilayered structure[45], which is not the case here (Fig. 2a,b). The intracellular membranes have a thickness consistent with those of modern thylakoids (two membranes separated by a lumen (measured at 12–16 nm in Fig. 4d in ref. 46 and at 14–18 nm in Figs. 1 and 2 in ref. 29)). These are interpreted as compressed, stacked, thylakoidal membranes preserved intracellularly and may represent a parallel and locally contorted arrangement[29].

Ultrathin sections of *N. majensis* from the Grassy Bay Formation show an ultrastructure that consists of an outer, electron-tenuous

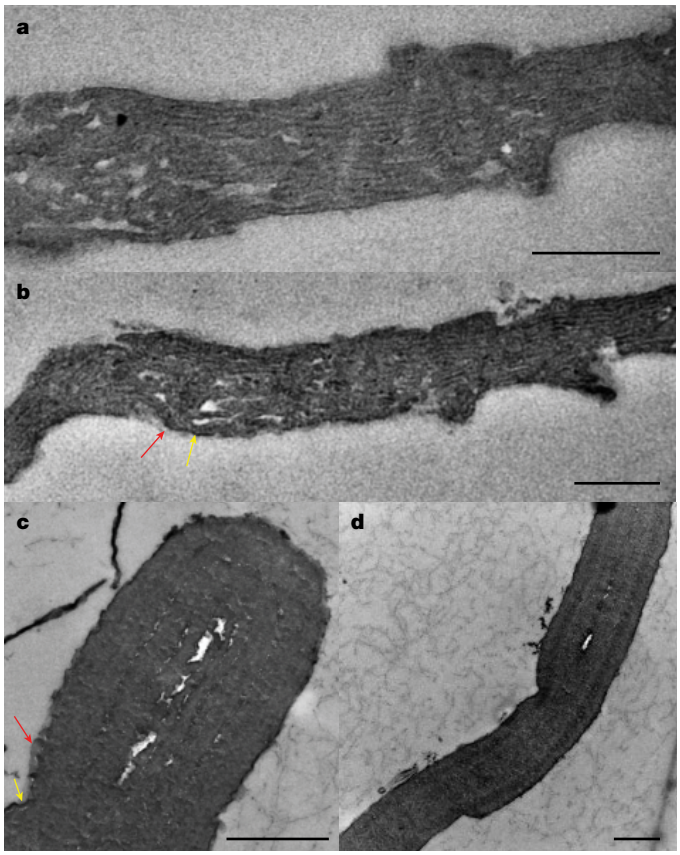


**Fig. 2 | TEM images of *N. majensis* from the McDermott Formation, Australia, and the Grassy Bay Formation, Canada. a**,**b**, Specimen from the McDermott Formation, Australia ($n = 2$). **a**, Well-defined contorted layers are interpreted as thylakoids. Each thylakoid comprises one medium-electron-dense layer surrounded by two electron-dense layers. **b**, Another part of the section, showing the electron-light outer layer (red arrow) overlying the very thin dark layers (yellow arrow), interpreted as the cell wall. **c**,**d**, Specimen from the Grassy Bay Formation, Canada ($n = 2$). End of the specimen (**c**) and intermediate region of the specimen (**d**), both showing well-preserved layers separated by white linear spaces (lumen) and interpreted as thylakoids with their concentric and parietal arrangement. The hole in the centre is the intracellular space. Possible partitions are visible between thylakoids, some possibly merged during diagenesis and burial compression (see also Extended Data Fig. 1b). The electron-light outer layer (red arrow in **c**) overlying the very thin dark layers (yellow arrow in **c**) is interpreted as the cell wall. *n*, number of specimens observed by TEM. Scale bars, 200 nm (**a**,**b**), 500 nm (**c**,**d**).

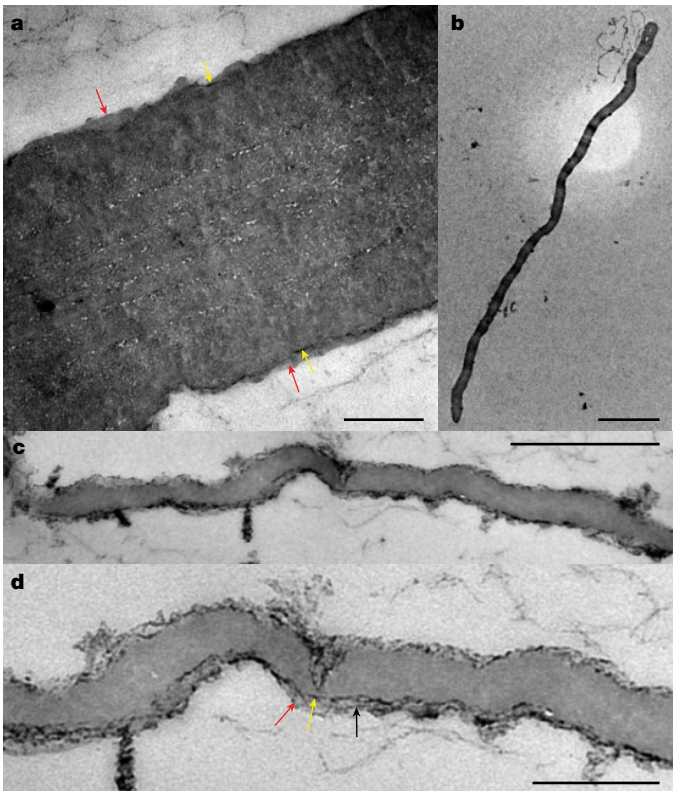


**Fig. 3 | TEM images of *N. majensis* from the Grassy Bay Formation, Canada, and the BIIc6 Formation, DRC. a**,**b**, Specimens from the Grassy Bay Formation ($n = 2$). **a**, The electron-light outer layer (red arrows) overlying the very thin dark layer (yellow arrows), both forming the cell wall; and the partition between stacked thylakoids, seen as lines of small, white holes. **b**, The complete transversal ultrathin section of a specimen, its length corresponding to microfossil width and its thickness corresponding to that of the flattened microfossil (Extended Data Fig. 4). **c**,**d**, Specimens from the BIIc6 Formation ($n = 2$). **c**, A homogeneous, medium-dense, inner layer surrounded by the outer wall. **d**, The outer wall comprises an electron-light outer layer (red arrow) that appears to be fibrous (black arrow) overlying the very thin dark layer (yellow arrow). Scale bars, 200 nm (**a**,**d**), 5 µm (**b**), 500 nm (**c**).

layer and a thin, dark layer surrounding a set of four to six uninterrupted, electron-dense concentric layers with sharp edges (Fig. 2c,d). The outer, electron-tenuous layer is sometimes poorly preserved and is underlain by a thin, dark layer, both forming the cell wall for a total thickness of up to 42 nm (Fig. 3a). The inner layers have thickness ranging between 18 and 97 nm (Extended Data Figs. 1 and 2 and Extended Data Table 1), except for the larger, outermost, inner layer with a thickness of approximately 200 nm (Fig. 3a). Larger layers (over 20 nm) probably correspond to merging of several membranes during burial, compression and diagenesis (Extended Data Fig. 1b). Moreover, larger layers have been observed in the modern cyanobacterium *Spirulina major* (PCC 6313), for which thylakoids may fill almost the whole cell with a 4.75–6.25-fold thicker subperipheral layer consisting of tightly stacked membranes[29]. All of these intracellular layers are concentric, uninterrupted and show a parietal arrangement (Fig. 2c,d). Such a lamellar architecture is similar to the arrangement of thylakoids in some cyanobacterial strains[29] and potentially represents the most primitive architecture of thylakoids[33]. Here again, the more complex ultrastructure of the chloroplast is not observed for these specimens. The combination of thickness, electron density and parietal arrangement of these inner layers is consistent with the presence of thylakoids preserved intracellularly within these fossil cells.

Raman microspectroscopic geothermometry shows that temperatures undergone by fossils in the diagenetic window were around 181 °C for the Shaler fossils and about 188 °C for the Tawallah fossils, consistent with the respective geological contexts and evidencing their syngenicity (Fig. 4)[26,40,47]. Despite the darker brown colour of the organic wall of *N. majensis* from the Shaler Group (Fig. 1c,d) compared with the light brown Tawallah specimens (Fig. 1a,b), their outer wall thicknesses and ultrastructures are similar and thus differences in colour do not result from differences in wall thickness, ultrastructure or temperature. The low burial temperature, together with their taphonomy in clay-rich shales and their recalcitrant lipidic composition, may explain the preservation of intracellular structures such as thylakoids within recalcitrant cell walls. Organic-walled microfossils can be preserved compressed in shales as old as 3.2 Ga and withstand acid demineralization[48]. The ultrastructure of cell walls can be variably preserved within single Proterozoic specimens (for example, ref. 25) as observed here, and thylakoid membranes also withstand acid demineralization of fossil Holocene mats[38] and may show sharp edges compared with ill- to well-defined cell walls following acetolysis of modern

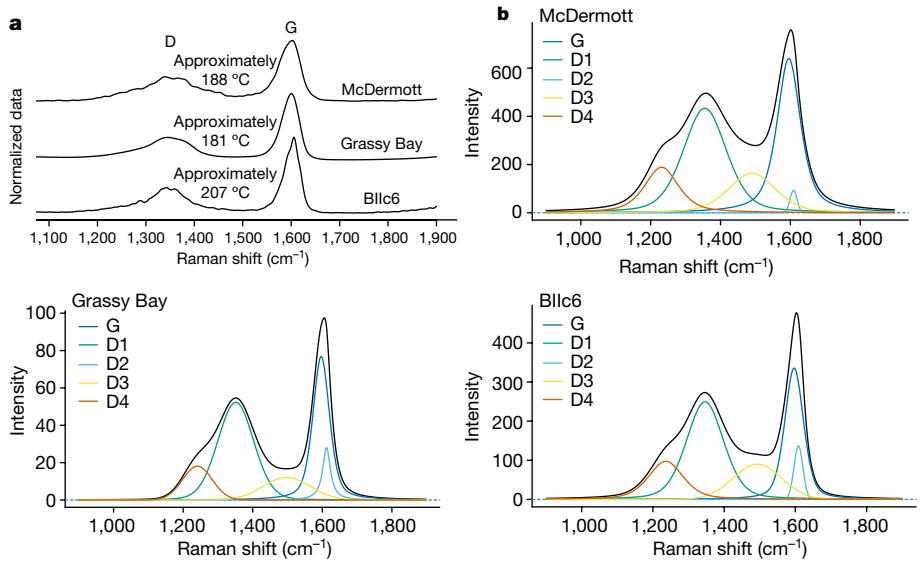


**Fig. 4 | Raman microspectroscopy of isolated *N. majensis* specimens.** **a**, Representative Raman spectra of *N. majensis* specimens from the three geological formations, representing the mean spectrum for each map. Palaeothermometry temperatures were calculated using the Raman reflectance method[59] for each geological context (McDermott Formation, $n = 2{,}801$, mean 187.9 ± 11.3 °C; Grassy Bay Formation, $n = 604$, mean 180.9 ± 13.1 °C; BIIc6 Formation, $n = 3{,}112$, mean 206.8 ± 4.5 °C. *n*, number of spectra for each map. **b**, One representative spectrum deconvolution for one specimen from each formation. Intensities are in arbitrary units. G, graphite band; D1–D4, disordered carbon bands.

and Mesozoic fossil cyanobacteria[34]. Such exquisite preservation and arrangement of intracellular membranes provide direct evidence for oxygenic photosynthesis, and the absence of chloroplast implies that *N. majensis* specimens from both formations represent cyanobacteria rather than algae.

By contrast, *N. majensis* specimens from the Mbuji-Mayi Supergroup differ markedly in their ultrastructure (Fig. 3c,d). These specimens show a homogeneous, electron-tenuous inner layer filling the vesicle, the cell lumen is not visible between the compressed walls and there are no distinctive inner layers such as in *N. majensis* specimens from the two other formations. This inner layer is 43–114 nm thick and is surrounded by one thin, electron-dense layer that, itself, is surrounded by an electron-lucent layer. These two layers are interpreted as the cell wall, which shows variable thickness all around the section, ranging from 3 to 66 nm, and appears locally fibrous or laminated where it is thicker (Fig. 3d). These observations are not consistent with the presence of inner stacked thylakoidal membranes. Raman palaeothermometry shows that the temperature undergone by these fossils was roughly 207 °C, similar to or only slightly higher than that for the other studied localities, suggesting that these DRC specimens either might not have preserved thylakoids or might not have possessed them originally, or they may represent another microbial clade (Fig. 4).

## Other interpretations of *Navifusa* spp.

*Navifusa* morphospecies gather dozens of microfossils with similar morphology and variable size, with a stratigraphic range from the Palaeoproterozoic to the Carboniferous[39,49]. Such ellipsoidal or cylindrical, smooth-walled, unornamented form is very simple and widespread in a large number of clades such as bacteria, microalgae and other protists, or fragmented eukaryotic multicellular organisms. This makes the interpretation of *Navifusa* microfossils ambiguous[22] because it could represent distinct lineages among prokaryotes and eukaryotes. The morphogenus *Navifusa* presents a morphology similar to that of other microfossils called *Archaeoellipsoides*[39] that are preserved silicified tridimensionally in chert[50]. These silicified microfossils are commonly interpreted as akinetes when associated with short trichomes interpreted as resulting from akinete germination[51,52], but see ref. 22. Akinetes are specialized dormant cells of nostocalean cyanobacteria produced under harsh environmental conditions[53]. One Devonian *Navifusa* species shows a longitudinal and trochospiral excystment structure and was interpreted as a eukaryotic alga[49]. Some larger Proterozoic specimens (300–550 µm long and 190–375 µm wide) were interpreted as probable eukaryotes[54]. Although the morphology and size of *Navifusa* spp. are coherent with several interpretations, the cellular ultrastructure permits discrimination of these hypothetic taxonomic placements. Indeed, modern cyanobacterial akinetes show an ultrastructure different from that observed in our fossil material[55], with a cell wall surrounded by a multilayered extracellular envelope of varying electron density[56] and reduced thylakoids[55]. However, the layers of the envelope may differ between species of cyanobacteria because in some strains the akinete envelope is an extracellular polysaccharidic matrix covering a thin glycolipid layer[55,56]. Such akinete ultrastructure clearly differs from that exhibited by the fossil specimens of the Shaler Supergroup and Tawallah Group studied here, which do possess well-developed inner layers interpreted as thylakoids with similar electron density and thickness but no multilayered extracellular envelope. Moreover, some modern cyanobacterial species have an ellipsoidal morphology similar to *N. majensis* with large dimensions, such as *Cyanothece major* (30–70 × 28–52 µm$^2$) or *Cyanothece aeruginosa* (10–50 × 10–38 µm$^2$)[7].

## Implications of preserved thylakoids

Although thylakoid arrangements do not permit pinpointing of a specific clade of cyanobacteria due to convergence within this clade, a parietal arrangement was proposed as the earliest to appear in thylakoid-bearing clades[29]. The discovery of preserved thylakoids in *N. majensis* from both the Shaler Supergroup and Tawallah Group provides direct evidence for oxygenic photosynthesis, for a cyanobacterial affinity and for a metabolically active vegetative cell rather than a cyst (akinete) stage for these specimens. As illustrated by the difference in ultrastructure of *Navifusa* specimens from the three geological successions despite similar morphologies, ultrastructural analyses of enigmatic microfossils, although scarcely applied, is a powerful tool for deciphering their palaeobiology, metabolism and taxonomic identity.

The fossiliferous levels of the (approximately) 1.75 Ga McDermott Formation studied here were deposited in anoxic, shallow-marine-to-evaporitic coastal environments based on sedimentology and trace elements and mineralogical palaeoredox proxies[40,47]. Our study provides direct evidence for the presence of metabolically active cyanobacteria performing oxygenic photosynthesis. It implies that the well-preserved microfossil record might capture low-concentration or local or short-term oxygenation events that are difficult to detect by geochemical proxies. Indeed, the detection limit of the latter, or the lack of temporal and spatial resolution of the averaging sedimentary record or balance between the biological source and sink of oxygen, might impede the recognition of oxygen traces in the rock record. Our approach thus offers a new, highly sensitive and complementary redox proxy for probing micro-oxic oases on the early Earth, where eukaryogenesis may have taken place close to oxygen-producing cyanobacteria and where early eukaryotes diversified[57,58]. Our study findings also imply that ultrastructural analyses of early fossil protists might show the presence of thylakoids enclosed in chloroplast and help to constrain the timing of plast endosymbiosis and the early evolution of eukaryotic algae.

The discovery of preserved thylakoids within *N. majensis* reported here provides direct evidence for a minimum age of about 1.75 Ga for the divergence between thylakoid-bearing and thylakoid-less cyanobacteria. By probing the older fossil record, it may also allow testing of the hypothesis that the emergence of thylakoid membranes may have contributed to the rise in oxygen around the GOE, and to the permanent oxygenation of the early Earth. We predict that similar ultrastructural analyses of well-preserved microfossils might expand the geological record of oxygenic photosynthesizers, and of early, weakly oxygenated ecosystems in which complex cells developed.

## Online content

Any methods, additional references, Nature Portfolio reporting summaries, source data, extended data, supplementary information, acknowledgements, peer review information; details of author contributions and competing interests; and statements of data and code availability are available at https://doi.org/10.1038/s41586-023-06896-7.


1. Sánchez-Baracaldo, P., Bianchini, G., Wilson, J. D. & Knoll, A. H. Cyanobacteria and biogeochemical cycles through Earth history. *Trends Microbiol.* **30**, 143–157 (2022).
2. Ostrander, C. M., Johnson, A. C. & Anbar, A. D. Earth's first redox revolution. *Annu. Rev. Earth Planet. Sci.* **49**, 337–366 (2021).
3. Wilmeth, D. T. et al. Evidence for benthic oxygen production in Neoarchean lacustrine stromatolites. *Geology* **50**, 907–911 (2022).
4. Slotznick, S. P. et al. Reexamination of 2.5-Ga "Whiff" of oxygen interval points to anoxic ocean before GOE. *Sci. Adv.* **8**, eabj7190 (2022).
5. Demoulin, C. F. et al. Cyanobacteria evolution: insight from the fossil record. *Free Rad. Biol. Med.* **140**, 206–223 (2019).
6. Rippka, R., Waterbury, J. & Cohen-Bazire, G. A cyanobacterium which lacks thylakoids. *Arch. Microbiol.* **100**, 419–436 (1974).
7. Komarek, J. & Anagnostidis, K. in *Freshwater Flora of Central Europe* Vol. 19, (ed. Moltmann, U. G.) 34–36 (Spektrum Akademischer, 2008).
8. Cavalier-Smith, T. The neomuran origin of archaebacterial, the negibacterial root of the universal tree and bacterial megaclassification. *Int. J. Syst. Evol. Microbiol.* **52**, 7–76 (2002).
9. Shih, P. M., Hemp, J., Ward, L. M., Matzke, N. J. & Fischer, W. W. Crown group Oxyphotobacteria postdate the rise of oxygen. *Geobiology* **15**, 19–29 (2017).
10. Rahmatpour, N. et al. A novel thylakoid-less isolate fills a billion-year gap in the evolution of cyanobacteria. *Curr. Biol.* **31**, 2857–2867 (2021).
11. Fournier, G. P. et al. The Archean origin of oxygenic photosynthesis and extant cyanobacterial lineages. *Proc. R. Soc. Lond. B Biol. Sci.* **288**, 20210675 (2021).
12. Hofmann, H. J. Precambrian microflora, Belcher Islands, Canada: significance and systematics. *J. Paleontol.* **50**, 1040–1073 (1976).
13. Hodgskiss, M. S. et al. New insights on the Orosirian carbon cycle, early Cyanobacteria, and the assembly of Laurentia from the Paleoproterozoic Belcher Group. *Earth Planet. Sci. Lett.* **520**, 141–152 (2019).
14. Jabłońska, J. & Tawfik, D. S. The evolution of oxygen-utilizing enzymes suggests early biosphere oxygenation. *Nat. Ecol. Evol.* **5**, 442–448 (2021).
15. Cardona, T., Sánchez-Baracaldo, P., Rutherford, A. W. & Larkum, A. W. D. Early Archean origin of Photosystem II. *Geobiology* **17**, 127–150 (2019).
16. Sánchez-Baracaldo, P. & Cardona, T. On the origin of oxygenic photosynthesis and cyanobacteria. *New Phytol.* **225**, 1440–1446 (2020).
17. Blank, C. E. & Sánchez-Baracaldo, P. Timing of morphological and ecological innovations in the cyanobacteria a key to understand the rise in atmospheric oxygen. *Geobiology* **8**, 1–23 (2010).
18. Schirrmeister, B. E., Gugger, M. & Donoghue, P. C. Cyanobacteria and the Great Oxidation Event: evidence from genes and fossils. *Palaeontology* **58**, 769–785 (2015).
19. Shih, P. M. et al. Biochemical characterization of predicted Precambrian RuBisCO. *Nat. Commun.* **7**, 10382 (2016).
20. Schwartz, R. M. & Dayhoff, M. O. Origins of prokaryotes, eukaryotes, mitochondria, and chloroplasts. *Science* **199**, 395–403 (1978).
21. Golubic, S. & Hofmann, H. J. Comparison of Holocene and mid-Precambrian Entophysalidaceae (Cyanophyta) in stromatolitic algal mats: cell division and degradation. *J. Paleontol.* **50**, 1074–1082 (1976).
22. Butterfield, N. J. Proterozoic photosynthesis – a critical review. *Palaeontology* **58**, 953–972 (2015).
23. Sergeev, V. N. Microfossils in cherts from the middle riphean (mesoproterozoic) Avzyan Formation, southern ural Mountains, Russian federation. *Precambrian Res.* **65**, 231–254 (1994).
24. Zhang, Y. Proterozoic stromatolitic micro-organisms from Hebei, North China: cell preservation and cell division. *Precambrian Res.* **38**, 165–175 (1988).
25. Javaux, E. J., Knoll, A. H. & Walter, M. R. TEM evidence for eukaryotic diversity in mid-Proterozoic oceans. *Geobiology* **2**, 121–132 (2004).
26. Loron, C. C., Rainbird, R. H., Turner, E. C., Greenman, J. W. & Javaux, E. J. Organic-walled microfossils from the late Mesoproterozoic to early Neoproterozoic lower Shaler Supergroup (Arctic Canada): diversity and biostratigraphic significance. *Precambrian Res.* **321**, 349–374 (2019).
27. Shimoni, E., Rav-Hon, O., Ohad, I., Brumfeld, V. & Reich, Z. Three-dimensional organization of higher-plant chloroplast thylakoid membranes revealed by electron tomography. *Plant Cell* **17**, 2580–2586 (2005).
28. Gonzalez-Esquer, C. R. et al. Cyanobacterial ultrastructure in light of genomic sequence data. *Photosynth. Res.* **129**, 147–157 (2016).
29. Mareš, J., Strunecký, O., Bučinská, L. & Wiedermannova, J. Evolutionary patterns of thylakoid architecture in cyanobacteria. *Front. Microbiol.* **10**, 277 (2019).
30. Mareš, J. et al. The primitive thylakoid-less cyanobacterium *Gloeobacter* is a common rock-dwelling organism. *PLoS ONE* **8**, e66323 (2013).
31. Nelissen, B., Van de Peer, Y., Wilmotte, A. & De Wachter, R. An early origin of platids within the cyanobacterial divergence is suggested by evolutionary trees based on complete 16S rRNA sequences. *Mol. Biol. Evol.* **12**, 1166–1173 (1995).
32. Raven, J. A. & Sànchez-Baracaldo, P. *Gloeobacter* and the implications of a freshwater origin of cyanobacteria. *Phycologia* **60**, 402–418 (2021).
33. Guéguen, N. & Maréchal, E. Origin of cyanobacterial thylakoids via a non-vesicvular glycolipid phase transition and their impact on the Great Oxygenation Event. *J. Exp. Bot.* **73**, 2721–2734 (2022).
34. Pacton, M., Gorin, G. E. & Fiet, N. Unravelling the origin of ultralaminae in sedimentary organic matter: the contribution of bacteria and photosynthetic organisms. *J. Sediment. Res.* **78**, 654–667 (2008).
35. Kremer, B., Kaźmierczak, J. & Środoń, J. Cyanobacterial-algal crusts from Late Ediacaran paleosols of the East European Craton. *Precambrian Res.* **305**, 236–246 (2018).
36. Schoenhut, K., Vann, D. R. & LePage, B. A. Cytological and ultrastructural preservation in Eocene *Metasequoia* leaves from the Canadian High Arctic. *Am. J. Bot.* **91**, 816–824 (2004).
37. Wang, X., Liu, W., Du, K., He, X. & Jin, J. Ultrastructural of chloroplasts in fossil *Nelumbo* from the Eocene of Hainan Island, South China. *Plant Syst. Evol.* **300**, 2259–2264 (2014).
38. Lepot, K. et al. Organic and mineral imprints in fossil photosynthetic mats of an East-Antarctic lake. *Geobiol.* **12**, 424–450 (2014).
39. Miao, L., Moczydłowska, M., Zhu, S. & Zhu, M. New record of organic-walled, morphologically distinct microfossils from the late Paleoproterozoic ChangCheng Group in the Yanshan Range, North China. *Precambrian Res.* **321**, 172–198 (2019).
40. Spinks, S. C., Schmid, S. & Pagès, A. Delayed euxinia in Paleoproterozoic intracontinental seas: vital havens for the evolution of eukaryotes. *Precambrian Res.* **287**, 108–114 (2016).
41. François, C. et al. Multi-method dating constrains the diversification of early 2 eukaryotes in the Proterozoic Mbuji-Mayi Supergroup of the D.R.Congo and the geological evolution of the Congo Basin. *J. Afr. Earth Sci.* **198**, 104785 (2023).
42. Baludikay, B. K., Storme, J. Y., François, C., Baudet, D. & Javaux, E. J. A diverse and exquisitely preserved organic-walled microfossil assemblage from the Meso–Neoproterozoic Mbuji-Mayi Supergroup (Democratic Republic of Congo) and implications for Proterozoic biostratigraphy. *Precambrian Res.* **281**, 166–18 (2016).
43. Pyatiletov, V. G. Yudoma complex microfossils from southern Yakutia. *Geol. Geofiz.* **7**, 8–20 (1980).
44. Hofmann, H. J. & Jackson, G. D. Shale-facies microfossils from the Proterozoic Bylot Supergroup, Baffin Island, Canada. *J. Paleontol.* **68**, 1–35 (1994).
45. Kirchhoff, H. Chloroplast ultrastructure in plants. *New Phytol.* **223**, 565–574 (2019).
46. Meng, L. et al. Measuring the dynamic response of the thylakoid architecture in plant leaves by electron microscopy. *Plant Direct.* **4**, e00280 (2020).
47. Spinks, S. C., Schmid, S., Pagés, A. & Bluett, J. Evidence for SEDEX-style mineralization in the 1.7 Ga Tawallah Group, McArthur basin, Australia. *Ore Geol. Rev.* **76**, 122–139 (2018).
48. Javaux, E. J., Marshall, C. P. & Bekker, A. Organic-walled microfossils in 3.2-billion-year-old shallow-marine siliciclastic deposits. *Nature* **463**, 934–938 (2010).
49. Fatka, O. & Brocke, R. Morphological variability and method of opening of the Devonian acritarch *Navifusa bacilla*. *Rev. Palaeobot. Palynol.* **148**, 108–123 (2008).
50. Horodyski, R. J. & Donaldson, J. A. Microfossils from the middle Proterozoic Dismal Lakes Groups, Arctic Canada. *Precambrian Res.* **11**, 125–159 (1980).
51. Golubic, S., Sergeev, V. N. & Knoll, A. H. Mesoproterozoic *Archaeoellipsoides*: akinetes of heterocystous cyanobacteria. *Lethaia* **28**, 285–298 (1995).
52. Tomitani, A., Knoll, A. H., Cavanaugh, C. M. & Ohno, T. The evolutionary diversification of cyanobacteria: molecular–phylogenetic and paleontological perspectives. *Proc. Natl Acad. Sci. USA* **103**, 5442–5447 (2006).

53. Kaplan-Levy, R. N., Hadas, O., Summers, M. L., Rücker, J. & Sukenik, A. in *Dormancy and Resistance in Harsh Environments* (eds Lubzens, E. et al.) 5–27 (Springer, 2010).
54. Sergeev, V. N., Knoll, A. H., Vorob'eva, N. G. & Sergeeva, N. D. Microfossils from the lower Mesoproterozoic Kaltasy Formation, East European Platform. *Precambrian Res.* **278**, 87–107 (2015).
55. Sukenik, A., Rücker, J. & Maldener, I. in *Cyanobacteria from Basic Science to Applications* (eds Mishra, A. K. et al.) 65–77 (Academic, 2019).
56. Perez, R., Forchhammer, K., Salerno, G. & Maldener, I. Clear differences in metabolic and porphological adaptations of akinetes of two *Nostocales* living in different habitats. *Microbiology* **162**, 214–223 (2016).
57. López-García, P. & Moreira, D. The Syntrophy hypothesis for the origin of eukaryotes revisited. *Nat. Microbiol.* **5**, 655–667 (2020).
58. Javaux, E. J. in *Encyclopedia of Astrobiology* (eds Gargaud, M. et al.), Ch. 538–4, 1–5 (Springer, 2021).
59. Baludikay, B. K. et al. Raman microspectroscopy, bitumen reflectance and illite crystallinity scale: comparison of different geothermometry methods on fossiliferous Proterozoic sedimentary basins (DR Congo, Mauritania and Australia). *Int. J. Coal Geol.* **191**, 80–94 (2018).

# Methods

### Sample preparation and extraction of microfossils

Fossil specimens were obtained from (1) the Kanshi SB13 drill core, BIIC Formation, DRC (detailed log and geology in ref. 42; datings in ref. 41); (2) outcrop sample 15RAT-021A1, Grassy Bay Formation, Shaler Supergroup, Canada (detailed log and geology in ref. 26); and (3) the GSD7 core, McDermott Formation, Tawallah Group, Northern Territories, Australia (detailed log and geology in ref. 40). Microfossils of *N. majensis* were extracted from their shale matrix following a procedure modified from Grey[60]. This modified procedure avoids centrifugation that could damage microfossils. Rock samples were cleaned and crushed before undergoing acid treatment. First, crushed samples were bathed in HCl 35% to remove carbonates then in a HF 60% bath to remove silicates and finally in hot HCl to remove neoformed fluorides. Organic residues were filtered and stored in Milli-Q water. These macerates were then used to prepare samples for electron microscopy and Raman microspectroscopy. All figures in the manuscript were created using Inkscape software 1.1.2.

### TEM

Six isolated microfossils (two each from the Shaler and Mbuji-Mayi Supergroups and the Tawallah Group) were pipetted under a Nikon Eclipse Ts2 inverted microscope and then embedded in 1% agarose. Agarose cubes containing microfossils were dehydrated in a graded ethanol series of 70, 90 and 100%. Following dehydratation, microfossils were progressively included within Spi-Pon 812 resin (ARALDITE/EMbed EMBEDDING KIT, Mollenhauer Formula, catalogue no. 13940). Resin inclusion started with two successive baths of propylene oxide, followed by a bath in a mix of propylene oxide and Spi-Pon 812 resin (1:1) and then a final bath in pure resin. Finally, microfossils in pure resin were heated over 2 days at 60 °C. No difference was observed between stained and unstained specimens. The resulting blocks were cut into transversal, ultrathin sections with an ultramicrotome Leica EM UC7 and these were then deposited on formvar-covered copper grids for observation. Samples were observed using a TEM Tecnai Spirit T12 with a voltage of 120 kV (M4I Division of Nanoscopy, University of Maastricht, The Netherlands).

### Raman microspectroscopy

Three microfossils (one specimen from each geological formation) were pipetted under a Nikon Eclipse Ts2 inverted microscope, deposited on ZnSe plates and air-dried for 24 h. They were then analysed using a Renishaw Invia Raman microspectrometer with an Air-ion-40 mW monochromatic 514 nm laser source (Early Life Traces & Evolution–Astrobiology Laboratory, University of Liège, Belgium). The laser was focused using an objective of ×100 to obtain a spot size of 1–2 µm. Spectra were acquired in static mode, enabling a range from 1 to 2,000 $cm^{-1}$ with a spectral resolution of 4 $cm^{-1}$ and centred at 1,150 $cm^{-1}$. Acquisitions were acquired at a laser power of 0.1%, an integration time of 1 s and using a 1,800 l $mm^{-2}$ grating that illuminates a charge-coupled device array detector of 1,040 × 256 pixels. Map spectra were finally processed with Renishaw Wire 4.2 software and RStudio 4.1.1 software. The thermal maturity of the kerogenous walls of specimens was estimated using the Raman reflectance method previously described[59]. Basic statistics (means and s.d.) were calculated using Microsoft Excel 2016.

### Reporting summary

Further information on research design is available in the Nature Portfolio Reporting Summary linked to this article.

## Data availability

All raw data are deposited in ULiege institutional open archive ORBi and can be accessed at https://hdl.handle.net/2268/308458. The folder 'morphometry' contains a table with measurements of microfossil lengths and widths; the folder 'Raman_RawData' contains raw maps; the folder 'Raman_TreatedData_Temperatures' contains tables with the treated data used to obtain temperatures (palaeothermometry - Raman reflectance T°C Rmc Ro); the folder 'Raw_TEM_images' contains raw TEM images of microfossil ultrastructure with scales. All tables are in .txt format.

60. Grey, K. A modified palynological preparation technique for the extraction of large Neoproterozoic acanthomorph acritarchs and other acid-insoluble microfossils. Western Australia Geological Survey, Record 1999/10 (1999).

**Acknowledgements** We thank the Royal Museum for Central Africa (Tervuren, Belgium) and D. Baudet for access to the Kanshi SB13 drill core; S. Spinks and M. Kunzmann (CSIRO Mineral Resources, Australia) for samples from the GSD7 drill core at the Darwin core facility (Australia); and the Geological Survey of Canada's Geomapping for Energy and Minerals programme, G. Halverson (McGill University, Canada), R. Rainbird (GSC, Canada), E. Turner (Laurentian University, Canada), T. Gibson (McGill University, Canada) and C. Loron (ULiege, Belgium and University of Edinburgh, UK) for sampling the Shaler Supergroup in the Northwest Territories of Arctic Canada. We thank M. Giraldo at the Early Life Traces & Evolution–Astrobiology laboratory and C. López-Iglesias and H. Duimel at the Microscopy CORE Lab (University of Maastricht) for technical support. FRS-FNRS-FWO EOS ET-Home (grant no. 30442502), ERC Stg ELiTE FP7/308074, an Agouron Institute geobiology grant and BELSPO BRAIN project B2/212/PI/PORTAL supported this project.

**Author contributions** C.F.D., Y.J.L. and E.J.J. conceived the study and interpreted the data. A.L. performed acid demineralization and prepared microfossil slides. C.F.D. and E.J.J. performed TEM sample preparation and observations. C.F.D. and E.J.J. prepared samples for Raman spectroscopy. C.F.D., Y.J.L. and E.J.J. performed Raman analyses. C.F.D., Y.J.L. and E.J.J. wrote the paper. E.J.J. supervised the project.

**Competing interests** The authors declare no competing interests.

**Additional information**
**Supplementary information** The online version contains supplementary material available at https://doi.org/10.1038/s41586-023-06896-7.
**Correspondence and requests for materials** should be addressed to Catherine F. Demoulin or Emmanuelle J. Javaux.
**Peer review information** *Nature* thanks Helmut Kirchhoff and the other, anonymous, reviewer(s) for their contribution to the peer review of this work.

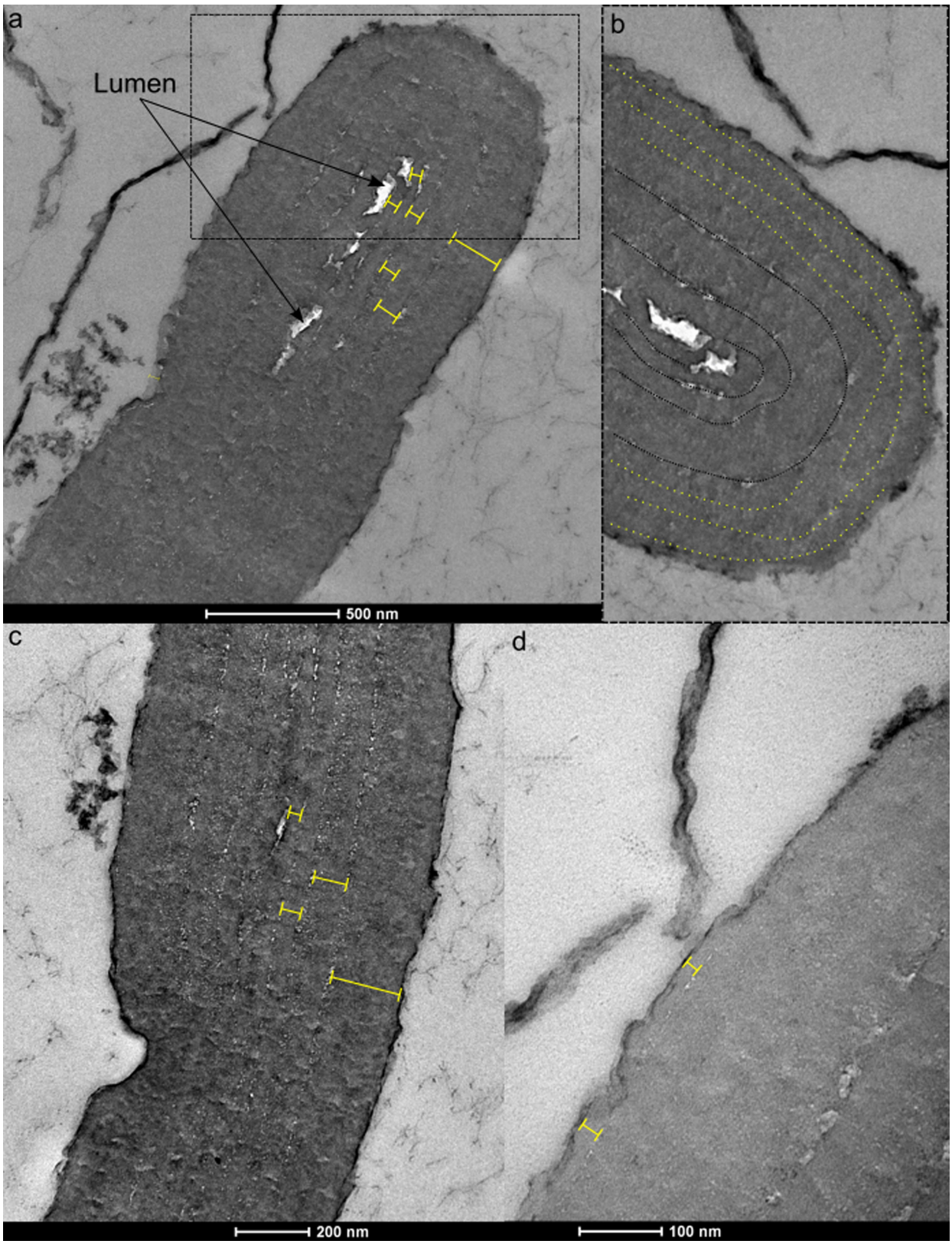


**Extended Data Fig. 1 | TEM pictures of a specimen of *Navifusa majensis*, from the Grassy Bay Formation (Shaler Supergroup, Canada).** Pictures a, c and d show the width and limits of each layer interpreted as stacked thylakoidal membranes that were measured. Measurements are compiled in Extended Data Table 1 below. Picture b is a zoom of the section through the microfossil rounded end in a (black box). The parietal arrangement is clearly visible (dotted black lines), as well as the variable thicknesses of stacked thylakoidal membranes, due to merging of several thylakoids during burial, compression and diagenesis, dotted yellow lines show possible limits of several layers in the ticker one. These TEM pictures are from the same specimen illustrated in Fig. 2c,d; 3a,b.

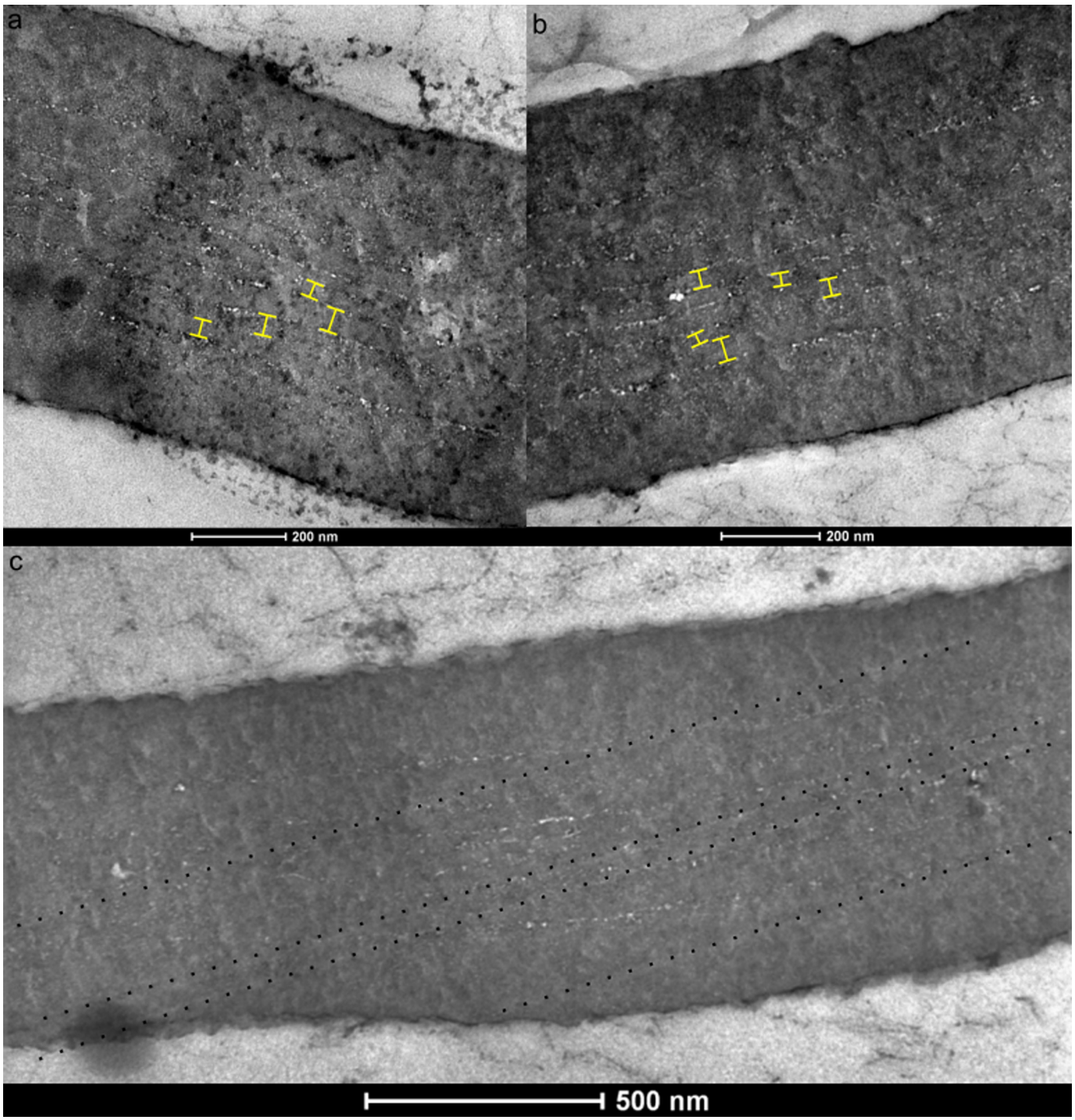


**Extended Data Fig. 2 | TEM pictures of the second specimen of *Navifusa majensis* from the Grassy Bay Formation (Shaler Supergroup, Canada).** Pictures a and b show some positions where thickness of layers were measured and clearly illustrate the limits of each layer interpreted as stacked thylakoidal membranes. Measures are summarized in the Extended Data Table 1 below. Picture c shows knife marks (dotted lines) creating artefacts on ultrathin sections. These knife marks are clearly distinguishable from limits of stacked thylakoidal layers. Picture c also shows that on a same ultrathin section, the limits between layers may be less clear, due to merging during burial and compression. n = 2 *N. majensis* for Grassy Bay Formation. "n" represents the number of specimens observed by TEM.

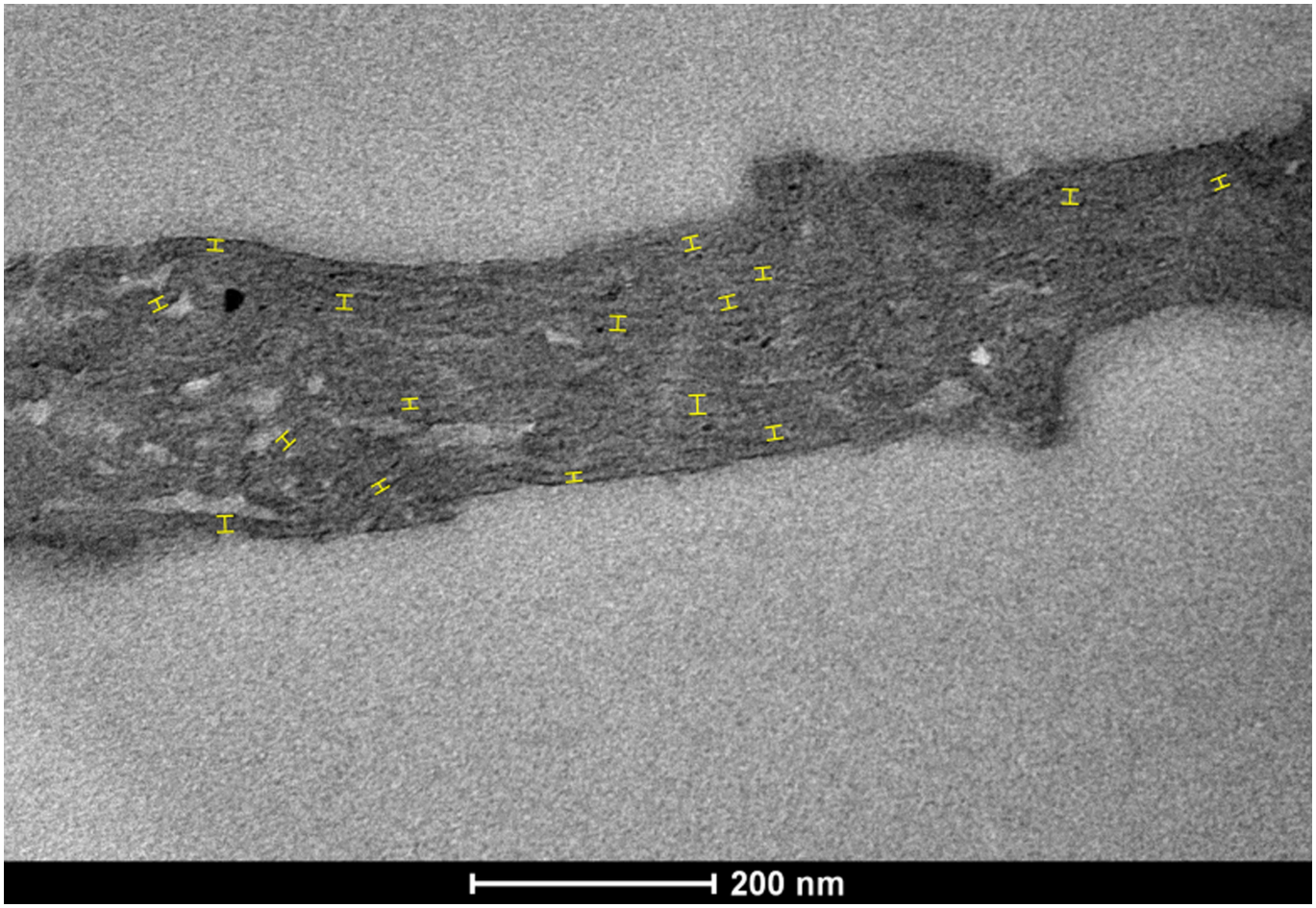


**Extended Data Fig. 3 | TEM picture of a specimen of *Navifusa majensis* from the McDermott Formation (Tawallah Group, Australia).** This picture shows the positions where the thylakoidal membranes are measured. Measurements are compiled in table S4 below. n = 2 *N. majensis* for McDermott Formation. "n" represents the number of specimens observed by TEM.

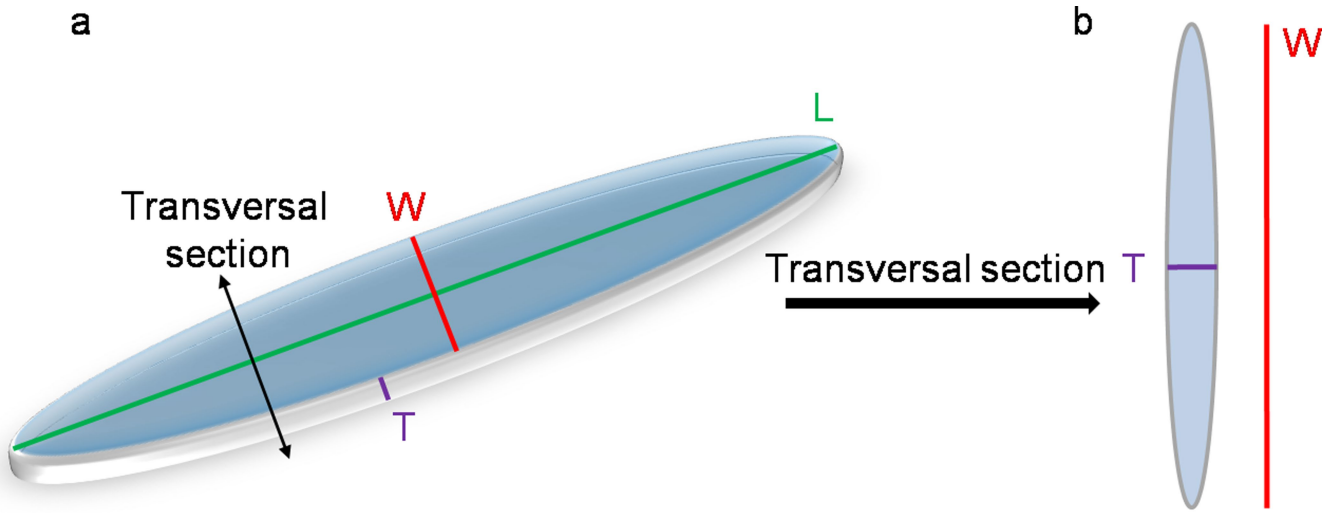


**Extended Data Fig. 4 | Schematic drawings showing how compressed microfossils were cut transversally for TEM observations.** a represents a whole flattened specimen of *Navifusa majensis*, with transversal section shown (black line). b represents a transversal TEM ultrathin section through the microfossil. The length of the ultrathin section in b corresponds to the width of the microfossil (red line in a and b), while the thickness of the ultrathin section corresponds to the thickness of the compressed microfossil (T in a and b). L: length of the whole microfossil; W: width; T: thickness.

**Extended Data Table 1 | Measurements of thickness of layers interpreted as stacked thylakoids in *Navifusa majensis* from both Shaler Supergroup (Extended Data Figs. 1 and 2) and Tawallah Group (Extended Data Fig. 3)**

| Extended Data Figures | 1a | 1c | 1d | 2a | 2b | 3 |
|---|---|---|---|---|---|---|
| Thickness (nm) | 55 | 30 | 18 | 40 | 30 | 10 |
| | 42 | 60 | 27 | 48 | 31 | 10 |
| | 55 | 90 | | 40 | 38 | 15 |
| | 69 | 190 | | 40 | 31 | 15 |
| | 97 | | | | 54 | 10 |
| | 194 | | | | | 10 |
| | | | | | | 10 |
| | | | | | | 15 |
| | | | | | | 10 |
| | | | | | | 15 |
| | | | | | | 13 |
| | | | | | | 15 |
| | | | | | | 20 |
| | | | | | | 15 |
| | | | | | | 15 |
| | | | | | | 10 |

nature portfolio

Corresponding author(s): Emmanuelle J. JAVAUX (ej.javaux@uliege.be)

Last updated by author(s): 6 November 2023

# Reporting Summary

Nature Portfolio wishes to improve the reproducibility of the work that we publish. This form provides structure for consistency and transparency in reporting. For further information on Nature Portfolio policies, see our Editorial Policies and the Editorial Policy Checklist.

## Statistics

For all statistical analyses, confirm that the following items are present in the figure legend, table legend, main text, or Methods section.

| n/a | Confirmed | |
|---|---|---|
| ☐ | ☒ | The exact sample size (*n*) for each experimental group/condition, given as a discrete number and unit of measurement |
| ☐ | ☒ | A statement on whether measurements were taken from distinct samples or whether the same sample was measured repeatedly |
| ☒ | ☐ | The statistical test(s) used AND whether they are one- or two-sided<br>*Only common tests should be described solely by name; describe more complex techniques in the Methods section.* |
| ☒ | ☐ | A description of all covariates tested |
| ☒ | ☐ | A description of any assumptions or corrections, such as tests of normality and adjustment for multiple comparisons |
| ☐ | ☒ | A full description of the statistical parameters including central tendency (e.g. means) or other basic estimates (e.g. regression coefficient) AND variation (e.g. standard deviation) or associated estimates of uncertainty (e.g. confidence intervals) |
| ☒ | ☐ | For null hypothesis testing, the test statistic (e.g. *F*, *t*, *r*) with confidence intervals, effect sizes, degrees of freedom and *P* value noted<br>*Give P values as exact values whenever suitable.* |
| ☒ | ☐ | For Bayesian analysis, information on the choice of priors and Markov chain Monte Carlo settings |
| ☒ | ☐ | For hierarchical and complex designs, identification of the appropriate level for tests and full reporting of outcomes |
| ☒ | ☐ | Estimates of effect sizes (e.g. Cohen's *d*, Pearson's *r*), indicating how they were calculated |

*Our web collection on statistics for biologists contains articles on many of the points above.*

## Software and code

Policy information about availability of computer code

| | |
|---|---|
| Data collection | Zeiss AxioVision SE64 Rel. 4.9.1 software, Renishaw Wire 4.2, software, R Studio 4.1.1, Inkscape software 1.1.2. (figures and tables drawing) |
| Data analysis | Renishaw Wire 4.2 software, R Studio 4.1.1, Microsoft Excel 2016 |

For manuscripts utilizing custom algorithms or software that are central to the research but not yet described in published literature, software must be made available to editors and reviewers. We strongly encourage code deposition in a community repository (e.g. GitHub). See the Nature Portfolio guidelines for submitting code & software for further information.

## Data

Policy information about availability of data

All manuscripts must include a data availability statement. This statement should provide the following information, where applicable:

- Accession codes, unique identifiers, or web links for publicly available datasets
- A description of any restrictions on data availability
- For clinical datasets or third party data, please ensure that the statement adheres to our policy

All processed data are included in the main draft. Microfossils' collection is curated in the Early Life Traces & Evolution-Astrobiology Lab (UR Astrobiology, ULiege). Data and material are available upon reasonable request to CFD and EJJ.

## Research involving human participants, their data, or biological material

Policy information about studies with human participants or human data. See also policy information about sex, gender (identity/presentation), and sexual orientation and race, ethnicity and racism.

| | |
|---|---|
| Reporting on sex and gender | NA |
| Reporting on race, ethnicity, or other socially relevant groupings | NA |
| Population characteristics | NA |
| Recruitment | NA |
| Ethics oversight | NA |

Note that full information on the approval of the study protocol must also be provided in the manuscript.

# Field-specific reporting

Please select the one below that is the best fit for your research. If you are not sure, read the appropriate sections before making your selection.

☐ Life sciences ☐ Behavioural & social sciences ☒ Ecological, evolutionary & environmental sciences

For a reference copy of the document with all sections, see nature.com/documents/nr-reporting-summary-flat.pdf

# Life sciences study design

All studies must disclose on these points even when the disclosure is negative.

| | |
|---|---|
| Sample size | *Describe how sample size was determined, detailing any statistical methods used to predetermine sample size OR if no sample-size calculation was performed, describe how sample sizes were chosen and provide a rationale for why these sample sizes are sufficient.* |
| Data exclusions | *Describe any data exclusions. If no data were excluded from the analyses, state so OR if data were excluded, describe the exclusions and the rationale behind them, indicating whether exclusion criteria were pre-established.* |
| Replication | *Describe the measures taken to verify the reproducibility of the experimental findings. If all attempts at replication were successful, confirm this OR if there are any findings that were not replicated or cannot be reproduced, note this and describe why.* |
| Randomization | *Describe how samples/organisms/participants were allocated into experimental groups. If allocation was not random, describe how covariates were controlled OR if this is not relevant to your study, explain why.* |
| Blinding | *Describe whether the investigators were blinded to group allocation during data collection and/or analysis. If blinding was not possible, describe why OR explain why blinding was not relevant to your study.* |

# Behavioural & social sciences study design

All studies must disclose on these points even when the disclosure is negative.

| | |
|---|---|
| Study description | *Briefly describe the study type including whether data are quantitative, qualitative, or mixed-methods (e.g. qualitative cross-sectional, quantitative experimental, mixed-methods case study).* |
| Research sample | *State the research sample (e.g. Harvard university undergraduates, villagers in rural India) and provide relevant demographic information (e.g. age, sex) and indicate whether the sample is representative. Provide a rationale for the study sample chosen. For studies involving existing datasets, please describe the dataset and source.* |
| Sampling strategy | *Describe the sampling procedure (e.g. random, snowball, stratified, convenience). Describe the statistical methods that were used to predetermine sample size OR if no sample-size calculation was performed, describe how sample sizes were chosen and provide a rationale for why these sample sizes are sufficient. For qualitative data, please indicate whether data saturation was considered, and what criteria were used to decide that no further sampling was needed.* |
| Data collection | *Provide details about the data collection procedure, including the instruments or devices used to record the data (e.g. pen and paper, computer, eye tracker, video or audio equipment) whether anyone was present besides the participant(s) and the researcher, and whether the researcher was blind to experimental condition and/or the study hypothesis during data collection.* |
| Timing | *Indicate the start and stop dates of data collection. If there is a gap between collection periods, state the dates for each sample cohort.* |

| | |
|---|---|
| Data exclusions | *If no data were excluded from the analyses, state so OR if data were excluded, provide the exact number of exclusions and the rationale behind them, indicating whether exclusion criteria were pre-established.* |
| Non-participation | *State how many participants dropped out/declined participation and the reason(s) given OR provide response rate OR state that no participants dropped out/declined participation.* |
| Randomization | *If participants were not allocated into experimental groups, state so OR describe how participants were allocated to groups, and if allocation was not random, describe how covariates were controlled.* |

# Ecological, evolutionary & environmental sciences study design

All studies must disclose on these points even when the disclosure is negative.

| | |
|---|---|
| Study description | morphological, ultrastructural and microchemical analyses of organic-walled microfossils |
| Research sample | The samples come from three geological formations in three different paleocontinents. Their choice was based on their very good preservation, the abondance of microfossil specimens, and the stratigraphic and geographic range. |
| Sampling strategy | We selected the best and complete specimens from three geological formations in three different paleocontinents to cover a stratigraphic and geographic range. |
| Data collection | C.F.D., Y.J.L. and E.J.J. conceived the study and interpreted the data. A.L. performed acid demineralization and prepared microfossils slides. C.F.D. and E.J.J. performed the TEM samples preparation and observations. C.F.D. and E.J.J. prepared samples for Raman spectroscopy. C.F.D.,Y.J.L. and E.J.J. performed Raman analyses. C.F.D., Y.J.L. and E.J.J. wrote the paper. E.J.J. supervised the project |
| Timing and spatial scale | Analyses of microfossils were conducted during the years 2021-22-23 (based on availability of equipment) |
| Data exclusions | no data have been excluded |
| Reproducibility | 6 microfossil specimens for TEM (2 AU, 2 CAN, 2 DRC) ; 3 microfossil specimens for Raman microspectroscopy (1 AU, 1 CAN, 1 DRC); 16 (AU), 22 (CAN), 13 (DRC) for morphometry. So a total of 60 specimens including analyzes of at least 2 specimens from each locality (TEM) and more for morphometry were studied to cover the size range and ultrastructural and chemical variability of the populations |
| Randomization | this is not relevant for our study since we studied specimens of the same taxon from 3 localities |
| Blinding | this is not relevant for our study since we studied specimens of the same taxon from 3 localities |

Did the study involve field work? ☐ Yes ☒ No

## Field work, collection and transport

| | |
|---|---|
| Field conditions | *Describe the study conditions for field work, providing relevant parameters (e.g. temperature, rainfall).* |
| Location | *State the location of the sampling or experiment, providing relevant parameters (e.g. latitude and longitude, elevation, water depth).* |
| Access & import/export | *Describe the efforts you have made to access habitats and to collect and import/export your samples in a responsible manner and in compliance with local, national and international laws, noting any permits that were obtained (give the name of the issuing authority, the date of issue, and any identifying information).* |
| Disturbance | *Describe any disturbance caused by the study and how it was minimized.* |

# Reporting for specific materials, systems and methods

We require information from authors about some types of materials, experimental systems and methods used in many studies. Here, indicate whether each material, system or method listed is relevant to your study. If you are not sure if a list item applies to your research, read the appropriate section before selecting a response.

## Materials & experimental systems

| n/a | Involved in the study |
|---|---|
| ☒ | ☐ Antibodies |
| ☒ | ☐ Eukaryotic cell lines |
| ☐ | ☒ Palaeontology and archaeology |
| ☒ | ☐ Animals and other organisms |
| ☒ | ☐ Clinical data |
| ☒ | ☐ Dual use research of concern |
| ☒ | ☐ Plants |

## Methods

| n/a | Involved in the study |
|---|---|
| ☒ | ☐ ChIP-seq |
| ☒ | ☐ Flow cytometry |
| ☒ | ☐ MRI-based neuroimaging |

## Antibodies

Antibodies used: *Describe all antibodies used in the study; as applicable, provide supplier name, catalog number, clone name, and lot number.*

Validation: *Describe the validation of each primary antibody for the species and application, noting any validation statements on the manufacturer's website, relevant citations, antibody profiles in online databases, or data provided in the manuscript.*

## Eukaryotic cell lines

Policy information about cell lines and Sex and Gender in Research

Cell line source(s): *State the source of each cell line used and the sex of all primary cell lines and cells derived from human participants or vertebrate models.*

Authentication: *Describe the authentication procedures for each cell line used OR declare that none of the cell lines used were authenticated.*

Mycoplasma contamination: *Confirm that all cell lines tested negative for mycoplasma contamination OR describe the results of the testing for mycoplasma contamination OR declare that the cell lines were not tested for mycoplasma contamination.*

Commonly misidentified lines (See ICLAC register): *Name any commonly misidentified cell lines used in the study and provide a rationale for their use.*

## Palaeontology and Archaeology

Specimen provenance: The microfossil material come from the collections of the Early Life Traces & Evolution-Astrobiology lab (UR Astrobiology-ULiege) and the taxonomy was described in taxonomy papers on fossil assemblages from DRC (Baludikay et al 2016; drill core samples from Royal Museum for Central Africa (Tervuren, Belgium)) and Arctic Canada (Loron et al 2019), and from an ongoing study (Javaux in prep) for the material from Australia (samples obtained from Darwin drill core collection) -see draft

Specimen deposition: The fossil material is part of the senior author (EJJ)'s collection at Early Life Traces & Evolution-Astrobiology lab (UR Astrobiology, ULiege) since 2013 (DRC), 2018 (CAN), 2017 (AU)

Dating methods: no new dates are provided

☐ Tick this box to confirm that the raw and calibrated dates are available in the paper or in Supplementary Information.

Ethics oversight: no ethical approval was required because the fossil material has been part of the senior author (EJJ)'s collection at Early Life Traces & Evolution-Astrobiology Lab at ULiege (EJJ)

Note that full information on the approval of the study protocol must also be provided in the manuscript.

## Animals and other research organisms

Policy information about studies involving animals; ARRIVE guidelines recommended for reporting animal research, and Sex and Gender in Research

Laboratory animals: *For laboratory animals, report species, strain and age OR state that the study did not involve laboratory animals.*

Wild animals: *Provide details on animals observed in or captured in the field; report species and age where possible. Describe how animals were caught and transported and what happened to captive animals after the study (if killed, explain why and describe method; if released, say where and when) OR state that the study did not involve wild animals.*

Reporting on sex: *Indicate if findings apply to only one sex; describe whether sex was considered in study design, methods used for assigning sex. Provide data disaggregated for sex where this information has been collected in the source data as appropriate; provide overall*

| | |
|---|---|
| | *numbers in this Reporting Summary. Please state if this information has not been collected. Report sex-based analyses where performed, justify reasons for lack of sex-based analysis.* |
| Field-collected samples | *For laboratory work with field-collected samples, describe all relevant parameters such as housing, maintenance, temperature, photoperiod and end-of-experiment protocol OR state that the study did not involve samples collected from the field.* |
| Ethics oversight | *Identify the organization(s) that approved or provided guidance on the study protocol, OR state that no ethical approval or guidance was required and explain why not.* |

Note that full information on the approval of the study protocol must also be provided in the manuscript.

## Clinical data

Policy information about clinical studies

All manuscripts should comply with the ICMJE guidelines for publication of clinical research and a completed CONSORT checklist must be included with all submissions.

| | |
|---|---|
| Clinical trial registration | *Provide the trial registration number from ClinicalTrials.gov or an equivalent agency.* |
| Study protocol | *Note where the full trial protocol can be accessed OR if not available, explain why.* |
| Data collection | *Describe the settings and locales of data collection, noting the time periods of recruitment and data collection.* |
| Outcomes | *Describe how you pre-defined primary and secondary outcome measures and how you assessed these measures.* |

## Dual use research of concern

Policy information about dual use research of concern

### Hazards

Could the accidental, deliberate or reckless misuse of agents or technologies generated in the work, or the application of information presented in the manuscript, pose a threat to:

| No | Yes | |
|---|---|---|
| ☒ | ☐ | Public health |
| ☒ | ☐ | National security |
| ☒ | ☐ | Crops and/or livestock |
| ☒ | ☐ | Ecosystems |
| ☒ | ☐ | Any other significant area |

### Experiments of concern

Does the work involve any of these experiments of concern:

| No | Yes | |
|---|---|---|
| ☒ | ☐ | Demonstrate how to render a vaccine ineffective |
| ☒ | ☐ | Confer resistance to therapeutically useful antibiotics or antiviral agents |
| ☒ | ☐ | Enhance the virulence of a pathogen or render a nonpathogen virulent |
| ☒ | ☐ | Increase transmissibility of a pathogen |
| ☒ | ☐ | Alter the host range of a pathogen |
| ☒ | ☐ | Enable evasion of diagnostic/detection modalities |
| ☒ | ☐ | Enable the weaponization of a biological agent or toxin |
| ☒ | ☐ | Any other potentially harmful combination of experiments and agents |

## Plants

| | |
|---|---|
| Seed stocks | *Report on the source of all seed stocks or other plant material used. If applicable, state the seed stock centre and catalogue number. If plant specimens were collected from the field, describe the collection location, date and sampling procedures.* |
| Novel plant genotypes | *Describe the methods by which all novel plant genotypes were produced. This includes those generated by transgenic approaches, gene editing, chemical/radiation-based mutagenesis and hybridization. For transgenic lines, describe the transformation method, the number of independent lines analyzed and the generation upon which experiments were performed. For gene-edited lines, describe the editor used, the endogenous sequence targeted for editing, the targeting guide RNA sequence (if applicable) and how the editor* |

*was applied.*

Authentication

*Describe any authentication procedures for each seed stock used or novel genotype generated. Describe any experiments used to assess the effect of a mutation and, where applicable, how potential secondary effects (e.g. second site T-DNA insertions, mosiacism, off-target gene editing) were examined.*

## ChIP-seq

### Data deposition

☐ Confirm that both raw and final processed data have been deposited in a public database such as GEO.

☐ Confirm that you have deposited or provided access to graph files (e.g. BED files) for the called peaks.

Data access links
*May remain private before publication.*

*For "Initial submission" or "Revised version" documents, provide reviewer access links. For your "Final submission" document, provide a link to the deposited data.*

Files in database submission

*Provide a list of all files available in the database submission.*

Genome browser session
(e.g. UCSC)

*Provide a link to an anonymized genome browser session for "Initial submission" and "Revised version" documents only, to enable peer review. Write "no longer applicable" for "Final submission" documents.*

### Methodology

Replicates

*Describe the experimental replicates, specifying number, type and replicate agreement.*

Sequencing depth

*Describe the sequencing depth for each experiment, providing the total number of reads, uniquely mapped reads, length of reads and whether they were paired- or single-end.*

Antibodies

*Describe the antibodies used for the ChIP-seq experiments; as applicable, provide supplier name, catalog number, clone name, and lot number.*

Peak calling parameters

*Specify the command line program and parameters used for read mapping and peak calling, including the ChIP, control and index files used.*

Data quality

*Describe the methods used to ensure data quality in full detail, including how many peaks are at FDR 5% and above 5-fold enrichment.*

Software

*Describe the software used to collect and analyze the ChIP-seq data. For custom code that has been deposited into a community repository, provide accession details.*

## Flow Cytometry

### Plots

Confirm that:

☐ The axis labels state the marker and fluorochrome used (e.g. CD4-FITC).

☐ The axis scales are clearly visible. Include numbers along axes only for bottom left plot of group (a 'group' is an analysis of identical markers).

☐ All plots are contour plots with outliers or pseudocolor plots.

☐ A numerical value for number of cells or percentage (with statistics) is provided.

### Methodology

Sample preparation

*Describe the sample preparation, detailing the biological source of the cells and any tissue processing steps used.*

Instrument

*Identify the instrument used for data collection, specifying make and model number.*

Software

*Describe the software used to collect and analyze the flow cytometry data. For custom code that has been deposited into a community repository, provide accession details.*

Cell population abundance

*Describe the abundance of the relevant cell populations within post-sort fractions, providing details on the purity of the samples and how it was determined.*

Gating strategy

*Describe the gating strategy used for all relevant experiments, specifying the preliminary FSC/SSC gates of the starting cell population, indicating where boundaries between "positive" and "negative" staining cell populations are defined.*

☐ Tick this box to confirm that a figure exemplifying the gating strategy is provided in the Supplementary Information.

# Magnetic resonance imaging

## Experimental design

| | |
|---|---|
| Design type | *Indicate task or resting state; event-related or block design.* |
| Design specifications | *Specify the number of blocks, trials or experimental units per session and/or subject, and specify the length of each trial or block (if trials are blocked) and interval between trials.* |
| Behavioral performance measures | *State number and/or type of variables recorded (e.g. correct button press, response time) and what statistics were used to establish that the subjects were performing the task as expected (e.g. mean, range, and/or standard deviation across subjects).* |

## Acquisition

| | |
|---|---|
| Imaging type(s) | *Specify: functional, structural, diffusion, perfusion.* |
| Field strength | *Specify in Tesla* |
| Sequence & imaging parameters | *Specify the pulse sequence type (gradient echo, spin echo, etc.), imaging type (EPI, spiral, etc.), field of view, matrix size, slice thickness, orientation and TE/TR/flip angle.* |
| Area of acquisition | *State whether a whole brain scan was used OR define the area of acquisition, describing how the region was determined.* |

Diffusion MRI ☐ Used ☐ Not used

## Preprocessing

| | |
|---|---|
| Preprocessing software | *Provide detail on software version and revision number and on specific parameters (model/functions, brain extraction, segmentation, smoothing kernel size, etc.).* |
| Normalization | *If data were normalized/standardized, describe the approach(es): specify linear or non-linear and define image types used for transformation OR indicate that data were not normalized and explain rationale for lack of normalization.* |
| Normalization template | *Describe the template used for normalization/transformation, specifying subject space or group standardized space (e.g. original Talairach, MNI305, ICBM152) OR indicate that the data were not normalized.* |
| Noise and artifact removal | *Describe your procedure(s) for artifact and structured noise removal, specifying motion parameters, tissue signals and physiological signals (heart rate, respiration).* |
| Volume censoring | *Define your software and/or method and criteria for volume censoring, and state the extent of such censoring.* |

## Statistical modeling & inference

| | |
|---|---|
| Model type and settings | *Specify type (mass univariate, multivariate, RSA, predictive, etc.) and describe essential details of the model at the first and second levels (e.g. fixed, random or mixed effects; drift or auto-correlation).* |
| Effect(s) tested | *Define precise effect in terms of the task or stimulus conditions instead of psychological concepts and indicate whether ANOVA or factorial designs were used.* |

Specify type of analysis: ☐ Whole brain ☐ ROI-based ☐ Both

| | |
|---|---|
| Statistic type for inference (See Eklund et al. 2016) | *Specify voxel-wise or cluster-wise and report all relevant parameters for cluster-wise methods.* |
| Correction | *Describe the type of correction and how it is obtained for multiple comparisons (e.g. FWE, FDR, permutation or Monte Carlo).* |

## Models & analysis

| n/a | Involved in the study |
|---|---|
| ☐ | ☐ Functional and/or effective connectivity |
| ☐ | ☐ Graph analysis |
| ☐ | ☐ Multivariate modeling or predictive analysis |

| | |
|---|---|
| Functional and/or effective connectivity | *Report the measures of dependence used and the model details (e.g. Pearson correlation, partial correlation, mutual information).* |
| Graph analysis | *Report the dependent variable and connectivity measure, specifying weighted graph or binarized graph,* |

| | |
|---|---|
| Graph analysis | *subject- or group-level, and the global and/or node summaries used (e.g. clustering coefficient, efficiency, etc.).* |
| Multivariate modeling and predictive analysis | *Specify independent variables, features extraction and dimension reduction, model, training and evaluation metrics.* |